M3LW-13OR0402054

Light Water Reactor Sustainability Program

Modeling Strategy to Assess Radiation Induced Segregation and Phase Stability in Austenitic Steels in Light Water Reactors During Extended services

June 30, 2013

U.S. Department of Energy

Office of Nuclear Energy

M3LW-13OR0402054

Modeling Strategy to Assess Radiation Induced Segregation and Phase Stability in Austenitic Steels in Light Water Reactors During Extended service:

Leland Barnard (University of Wisconsin, Madison)
Dane Morgan (University of Wisconsin, Madison)
Brian Wirth (University of Tennessee, Knoxville)

June 30, 2013

Prepared for the
U.S. Department of Energy
Office of Nuclear Energy

CONTENTS

FIGURES

SUMMARY

This report has been assembled to address the first milestone of the project entitled "Modeling Strategy to Assess Radiation Induced Segregation and Phase Stability in Austenitic Steels in Light Water Reactors during extended service," which was defined as follows:

"Milestone 1: Report summarizing available thermodynamic and kinetic properties of Ni, Mn, and Si in austenitic stainless steels in the literature and prioritizing ab-intio and atomistic calculations to fill gaps."

The goal of this document is to provide a high level assessment of existing models and data sets that describe thermodynamic and kinetic aspects of the precipitation of Mn-Ni-Si rich phases in austenitic stainless, as well as describe planned atomistic simulations. Furthermore, an approach for incorporating these models into a framework for understanding and predicting Mn-Ni-Si rich phase precipitation in a light water reactor environment is outlined.

Section 1 provides a background summary of the thermodynamic and kinetic models and information that are pertinent to the nucleation, growth, and coarsening of second phase precipitates under irradiation. Section 2 assesses the availability of these models and data in the Fe-Cr-Ni-Mn-Si system and highlights gaps where these existing resources might be insufficient. Section 3 describes available computational tools and methods that could be employed to address the gaps identified in section 2, with an emphasis on ab-initio and atomistic calculations and simulation tools. Finally, section 4 outlines a proposed framework that incorporates the models summarized in this report to create a first thermodynamic and kinetic model for describing the precipitation of Mn-Ni-Si rich phases in austenitic stainless steels under light water reactor operating conditions.

ACKNOWLEDGEMENTS

This research was sponsored by the U.S. Department of Energy, Office of Nuclear Energy, for the Light Water Reactor Sustainability Research and Development effort.

1. BACKGROUND

1.1 Experimental Studies of Mn-Ni-Si Precipitation in Austenitic Steels

Many researchers have observed the appearance of Ni-Si and Mn-Ni-Si precipitates in irradiated austenitic stainless steels [1-5], most commonly in alloys with high Ni concentration such as D9 and 316. Some of these precipitates have been identified as Ni_3Si or G-phase, an intermetallic phase with a nominal composition $M_6Ni_{16}Si_7$, where M is often Mn. Figure 1 depicts micrographs of Ni_3Si and G-phase [4] precipitates observed in irradiated austenitic alloys.

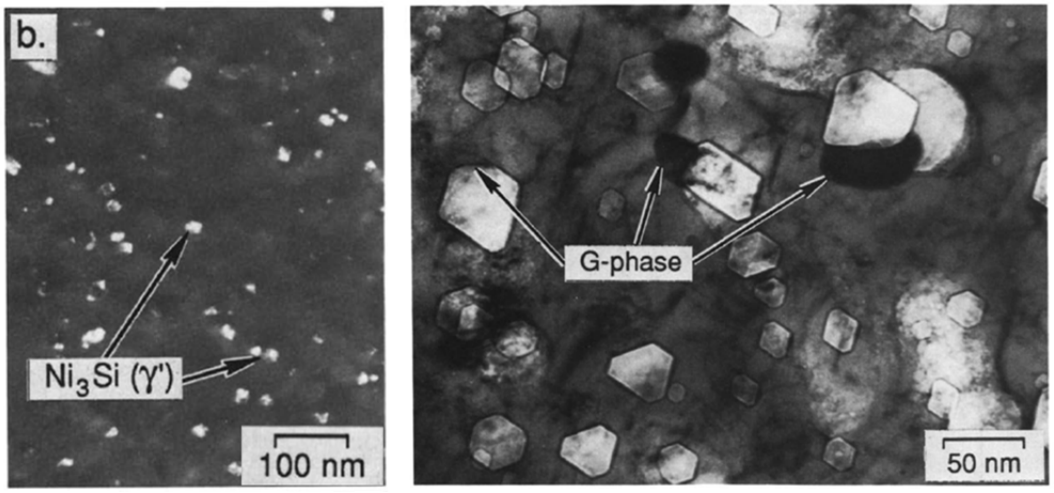

Figure 1: Micrographs of Ni_3Si and G-phase precipitates in irradiated austenitic alloys. From [4].

In both cases, the precipitates are strongly associated with voids, and Ni_3Si precipitation has been observed on or near dislocation loops as well [4]. This association with radiation-induced microstructural features suggests a significant radiation-induced component in the formation of these precipitates. The appearance of these phases is not generally observed under thermal aging at comparable temperatures, and their precipitation could have significant and unexpected consequences for the mechanical properties of the material. Understanding and predicting the precipitation of these phases is therefore crucial in forecasting the lifetime of these alloys under LWR operating conditions.

1.2 Modeling Mn-Ni-Si Precipitation in Austenitic Steels

Precipitation of second phases that occurs under irradiation can be broadly characterized using the following classification scheme:

1) ***Irradiation-induced precipitation***, which refers to the appearance of non-equilibrium phases under irradiation that would not appear under thermal aging, and that dissolve during post-irradiation heat treatment.

2) ***Irradiation-modified precipitation***, which refers to precipitates which are thermally stable but are significantly altered in their morphology or composition by the irradiation.

3) ***Irradiation-enhanced precipitation***, which refers to the precipitation of equilibrium phases at a rate that is significantly enhanced by the irradiation.

As a first step toward understanding and predicting the precipitation of Mn-Ni-Si phases under irradiation in austenitic stainless steels, we will seek to determine which of these categories best describes these precipitates. To this end we will establish a thorough thermodynamic description of the phase separation of Mn, Ni, and Si-rich phases from the austenite phase, using the CALPHAD (CALculation of PHAse Diagrams) methodology. This approach will help to isolate irradiation-enhanced precipitates from precipitates that are induced or significantly modified by the irradiation, as the later types of precipitates will not be predicted by thermodynamics alone. Xiong et al. [6] have used this approach to describe the precipitation of Mn-Ni-Si rich phases in reactor pressure vessel (RPV) steels with reasonable accuracy. Figure 2 compares the Mn-Ni-Si precipitate compositions in six irradiated RPV alloys as measured by Atom Probe Tomography (APT) and as predicted by CALPHAD, as well as the measured and predicted atomic fractions of precipitate phase. The good agreement between the model and experiment suggests that the precipitation of Mn-Ni-Si precipitates in the these RPVs is largely irradiation-enhanced precipitation, and that the thermodynamic model is of reasonable quality.

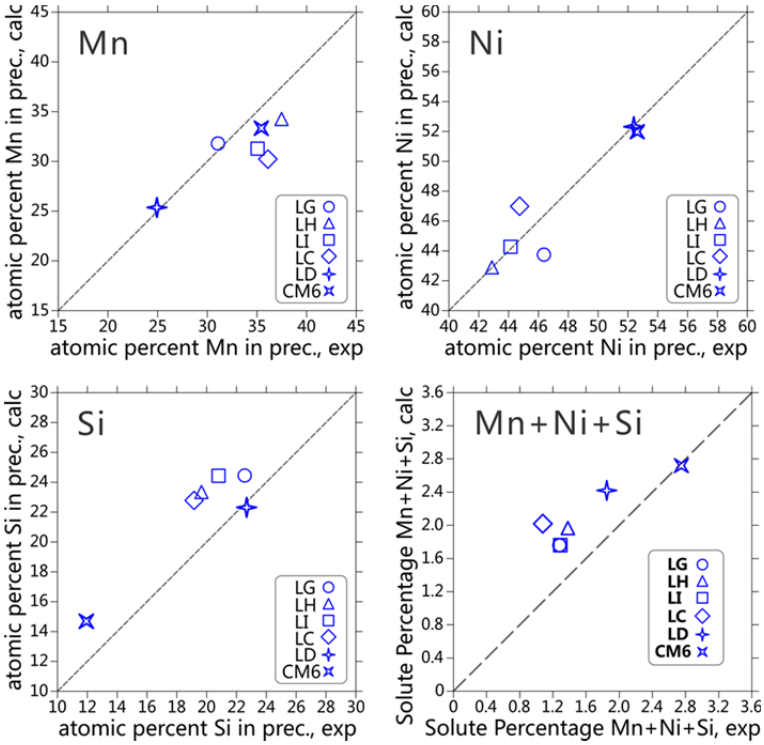

Figure 2: Measured Mn-Ni-Si precipitate compositions in 6 model reactor pressure vessel steels, and the final atomic percentage of the precipitate phase, compared to predictions of the CALPHAD model. Adapted from [6].

Additionally, this CALPHAD framework provides a foundation for the development of a kinetic theory of Mn-Ni-Si precipitate nucleation, growth, and coarsening in the classical nucleation theory (CNT) formalism. When combined with a detailed assessment of atomic mobilities in austenitic stainless steels, such a model can provide a reasonable approximation of

the kinetics of Mn-Ni-Si precipitation under simple thermal aging conditions. Radiation-enhanced precipitation can then be studied in a first approximation by incorporating radiation-enhanced solute diffusion into the CALPHAD-based CNT model. This approach has yielded accurate models for understanding and predicting radiation-enhanced precipitation in simpler systems. For example, results modeling Cu precipitation in Fe [7] are shown in figure 3, which depicts model predictions and experimental measurements of mean Cu precipitate size and precipitate number density as functions of time in an Fe-1.34 at% Cu alloy under electron irradiation at 290 °C. The excellent agreement shows that CALPHAD-based CNT modeling can be a powerful tool for studying radiation-enhanced precipitation.

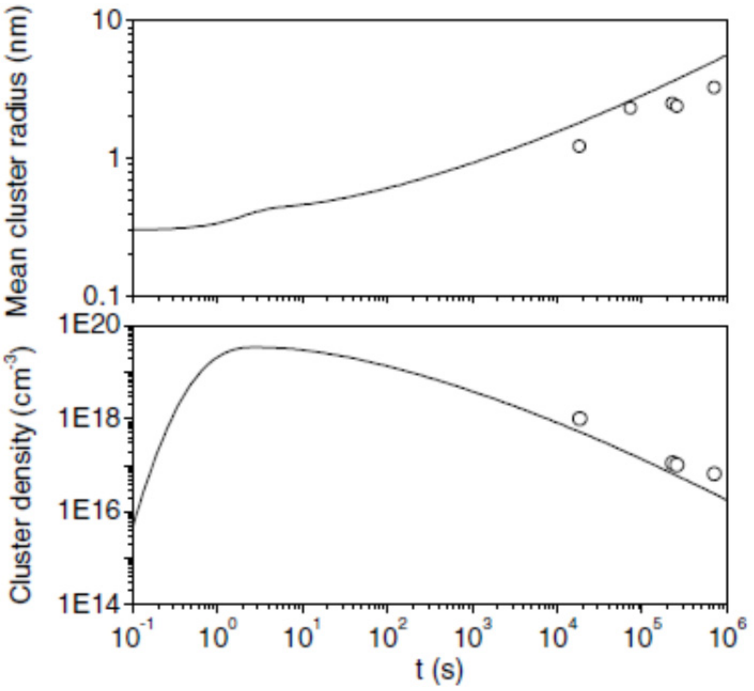

Figure 3: Comparison of model predictions and experimental measurements of mean Cu precipitate size and precipitate number number density as a function of time in an Fe-1.34 at% Cu alloy irradiated with electrons at 290 °C. From [7].

Finally, the presented modeling approach will allow us to begin studying the effects of radiation-induced segregation (RIS) on phase transformations. RIS can dramatically alter the alloy composition near certain microstructural features such as grain boundaries, potentially resulting in the precipitation of second phases that would not be thermodynamically stable at the nominal alloy composition. This is one mechanism by which radiation can induce precipitation, rather than only enhancing it. For example, extensive precipitation of Ni_3Si near grain boundaries in low Si Ni alloys has been attributed to local enrichment of Si due to RIS [8]. If the RIS tendencies of Mn, Ni, and Si are known, then the CALPHAD-based approach can be used to identify possible phases that might precipitate due to RIS-driven compositional changes.

Implementation of the modeling framework described above requires extensive thermodynamic and kinetic models and data for Mn, Ni, and Si in austenitic stainless steels, as well as a model for predicting the RIS behavior of these elements. The remaining sections in this

document will detail the availability of these models and data, and discuss potential gaps in the data sets that might be addressed with key atomistic calculations.

2. AVAILABILITY OF RELEVANT SOFTWARE, MODELS, AND DATA

2.1 CALPHAD databases

Extensive databases of thermodynamic models created specifically to describe Fe alloys and steels are available from multiple commercial parties. However, Mn-Ni-Si phases are not generally an emphasis in such databases and a description of the full Mn-Ni-Si ternary phase diagram is not typically included. The most applicable database for studying the precipitation of Mn-Ni-Si phases from austenitic stainless steels is therefore not one developed for Fe alloys but instead appears to the TCAL2 database, distributed and maintained by Thermo-Calc. Originally created to describe Al alloys, this database contains a full assessment of the Mn-Ni-Si ternary alloy system, as well as the Fe-Mn-Si, Fe-Mn-Ni, and Fe-Ni-Si ternary systems and all associated binary systems. Cr is a significant alloying component in austenitic steels as well, and a potential drawback of the TCAL2 database is the absence of an assessment of the Fe-Ni-Cr ternary system. However, the Cr-Fe, Cr-Ni, Cr-Si, and Cr-Mn binary systems are fully assessed. An accurate extrapolation to higher order systems including Cr should be possible from this collection of binary systems. We notes that TCAL2 also contains the element C, making the study of other precipitates beyond Mn-Ni-Si, e.g., the CrC_x precipitates, possible with the same database.

One area in which the TCAL2 database might prove insufficient is in the assessment of the fcc solid solution phase or possible fcc ordered compounds across the full Mn-Ni-Si composition space. The Mn-Ni-Si ternary phase diagram is characterized by many stoichiometric intermetallic compounds, and the fcc solid solution phase is metastable over nearly the entire composition range. Figure 4 depicts a section of the calculated Mn-Ni-Si phase diagram at 280 °C. The solid green region near the Ni corner is the extent of the region of stability of the fcc solid solution phase. The small range of fcc stability implies that very limited experimental data has been used in fitting the fcc energetics, which may lead to inaccuracies.

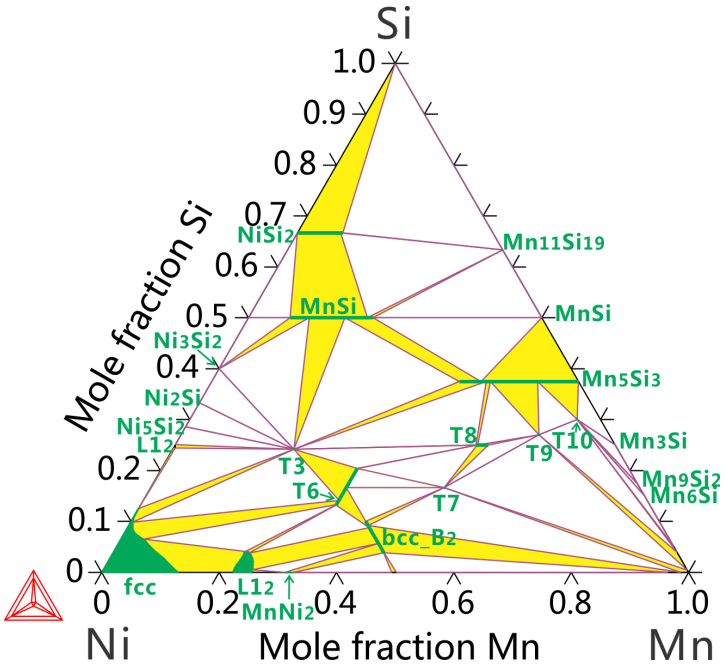

Figure 4: Calculated Mn-Ni-Si phase diagram at 280 °C. From [6].

Despite this limited region of stability, during the early stages of precipitation the Mn-Ni-Si rich particle nuclei are likely to be coherent with the austenite matrix. As such, an accurate description of the energetics of fcc Mn-Ni-Si over a wide composition range may be necessary to accurately model the formation of these nuclei.

We are also aware the Dr. Ying Yang at Oak Ridge National Laboratory (ORNL) is developing an austenitic CALPHAD database which is intended to include much of the thermodynamic information needed for studying the Ni-Mn-Si precipitation and be optimized specifically for nuclear steels (e.g., in terms of composition and temperature regions used in fitting) [9]. However, this database is not presently available and may take several years to complete. Furthermore, the public accessibility of this database is not clear. However, we are working with Dr. Yang to assure that any information we establish can be integrated into her database and that we make use of any thermodynamic data she is able to share with us.

2.2 Mobility and diffusion data

Accurate evaluation of composition and species dependent diffusion coefficients is necessary for both the implementation of CNT and the simulation of RIS. The diffusion of Fe, Ni, and Cr has been well studied and mobilities and chemical diffusion coefficients are available over a wide range of compositions and temperatures [10-13]. Theoretical values of the vacancy-mediated tracer diffusion coefficient have been calculated from ab-initio for Fe, Ni, and Cr [14], but similar calculations for Si and Mn have not been attempted. The diffusion coefficients of Si and Mn in stainless steels are less well established. Limited data is available for the diffusion of Mn [15] and Si [16] tracers in gamma Fe, and the activation energy of Si diffusion in the austenitic stainless steel alloy D9 [17].

Thermo-Calc also maintains databases of atomic mobilities which, when combined with an appropriate CALPHAD database, can be used to calculate chemical diffusion coefficients as a function of temperature and composition. The mobility database MOBAL2 is intended to be

used in conjunction with the CALPHAD database TCAL2, and can be used to calculate diffusion coefficients in the Fe-Mn, Fe-Ni, and Fe-Si binary systems over the full composition space, in the austenite phase. This database therefore provides the most extensive set of diffusion data for Mn, Ni, and Si, however it is still limited in the sense that extrapolations from binary systems must be made in order to calculate diffusion data in the full Fe-Ni-Cr-Mn-Si system.

Under irradiation, significant atomic transport can occur via a self-interstitial dumbbell mechanism, and interstitial diffusion coefficients are therefore an important component for calculating radiation-enhanced diffusion coefficients as well as for predicting RIS tendencies. No experimentally measured values of species-dependent interstitial diffusion coefficients in stainless steels are available, though the activation energy for self-interstitial migration has been measured across much of the Fe-Ni-Cr alloy space via resistivity recovery experiments [18].

2.3 RIS models and data

RIS of Fe, Ni, and Cr in stainless steels has been studied extensively and plentiful data exist on segregation as a function of alloy composition and irradiation conditions [8]. The modified inverse Kirkendall model (MIK) [19] was developed specifically to treat RIS of these three elements, and it can provide reasonably accurate Fe, Ni, and Cr RIS predictions for alloys across the entire Fe-Ni-Cr ternary alloy space. Figure 5 compares the measured Ni RIS to the predictions of the MIK model in a large number of Fe-Ni-Cr alloys.

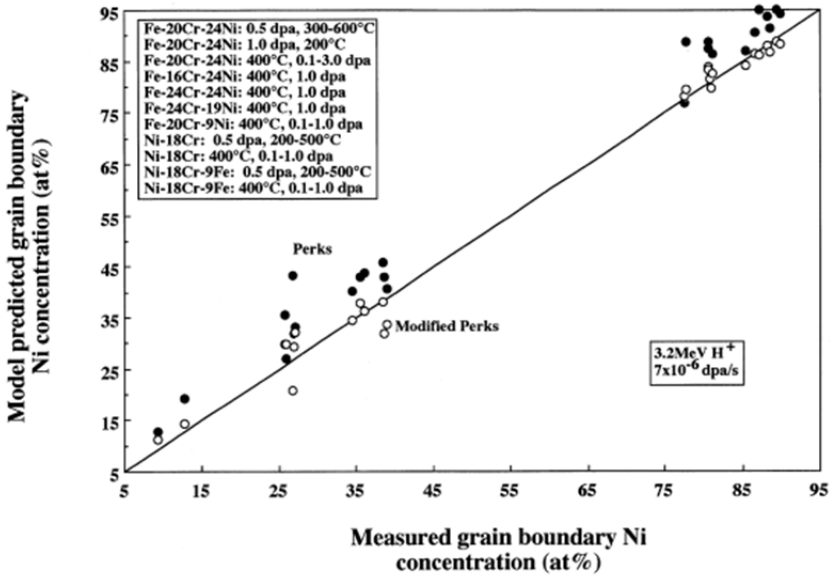

Figure 5: Comparison of measured Ni RIS to the predictions of the Perks and MIK (modified Perks) models. Reasonably good agreement is observed for a wide range of Fe-Ni-Cr alloys. From [19].

Si RIS has also been measured extensively in stainless steels [8, 20], and Fukuya et al. [21] have developed a multicomponent RIS model for austenitic stainless steels that can reproduce Si segregation profiles as a function of temperature and dose with reasonable accuracy. In figure 6, measured segregation profiles for Fe, Ni, Cr, and Si in alloy SUS316 irradiated to 3 dpa at 290 °C in a pressurized water reactor are compared to the predictions of the model of Fukuya et al.

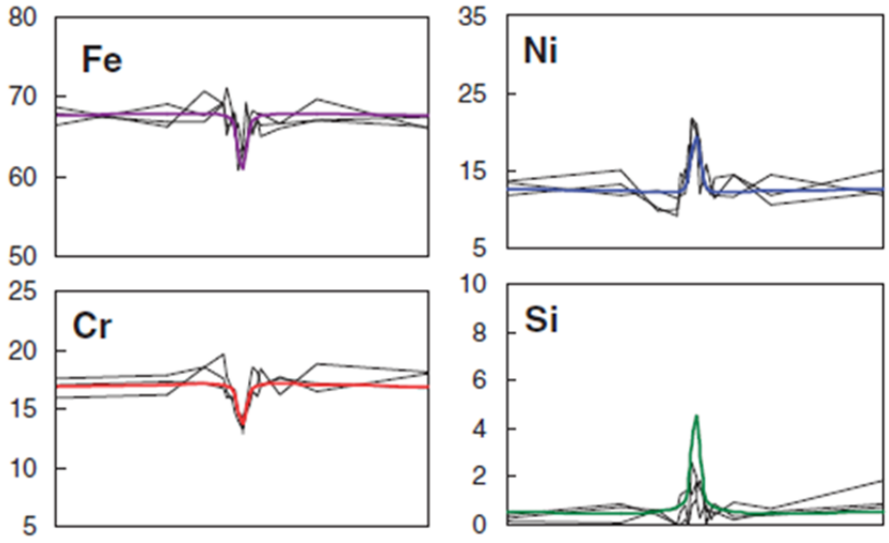

Figure 6: RIS profiles for Fe, Ni, Cr, and Si in SUS316 stainless steel irradiated to 3 dpa at 290 °C in a pressurized water reactor. Dark lines are experimental measurements, while colored curves are the predicted profiles of the model of Fukuya et al. From [21].

Very little segregation data exists for Mn, however there is some evidence that suggests similar RIS behavior to that of Cr [22]. Furthermore, there is currently no available RIS model for the prediction of Mn RIS in stainless steels, as any such model would be difficult to validate.

3. ATOMISTIC CALCULATIONS TO FILL GAPS

There are a number of areas in which in the available thermodynamic and kinetic models and data might be augmented using ab-initio-based atomistic calculations. First we consider thermodynamic data that can be obtained from ab-initio modeling.

While the CALPHAD database description of the metastable fcc Mn-Ni-Si free energy surface might be uncertain due to a lack of experimental data over much of the composition space, a description of a fixed fcc lattice phase diagram is an ideal application for grand canonical Monte Carlo simulations [23]. This is a simulation technique wherein arrangements of different types of atoms on a fixed lattice are sampled randomly with a probability weighted by their relative formation energies, with the purpose of finding the lowest energy arrangements. The results of these simulations can be used to construct a free energy curve at finite temperatures and ultimately compute the fcc Mn-Ni-Si phase diagram. Such a phase diagram can be validated against the portions of the experimental phase diagram where the fcc phase appears as the equilibrium state. The principal resource needed for such a phase diagram construction is a Hamiltonian that can accurately describe the formation energy of any arrangement of Mn, Ni, and Si atoms on an fcc lattice. This Hamiltonian can be constructed in the cluster expansion formalism [24-26], with input provided by a large suite of density functional theory (DFT) calculations of the formation energies of fcc Mn-Ni-Si structures.

Furthermore, some specific aspects of the thermodynamic data may turn out to be inconsistent with detailed precipitate observations or just more uncertain than desirable. For example, in discussions recently with Dr. Yang at ORNL, she brought up the issue of Fe alloying the Mn-Ni-Si G-phase. Previous APT studies has suggested Fe in G-phase precipitates, but this data was viewed as unreliable because of known problems of APT analysis erroneously

projecting host atoms into precipitates. We are exploring calculations of Fe energies in the G-phase to help assess the possibility of Fe alloying with G-phase precipitates.

DFT calculations can be used to improve the available kinetic and diffusion data as well. While experimentally measured diffusion coefficients in austenitic stainless steels are plentiful, they are most often measured at relatively high temperature, often over 1000 °C. Diffusion coefficients evaluated at LWR operating conditions are therefore often extrapolated over many hundreds of degrees. DFT calculations combined with analytical expressions known as multifrequency models [27] can be used as an alternative to calculate vacancy-mediated diffusion coefficients at low temperature.

Ab-initio calculations can also be used to access interstitial diffusion coefficients, which are generally unavailable by other means. Similar to vacancy-mediated diffusion, interstitial-mediated diffusion coefficients can be calculated by combining DFT-calculated atomic migration energies with analytical multifrequency expressions. An alternative approach is to simulate interstitial diffusion on an fcc lattice via ab-initio-based molecular dynamics and measure diffusion coefficients from the displacements of the atoms. This method has been used to determine, e.g., interstitial diffusion coefficients in Si [28] and in Ni-Cr alloys [29], as well as ion conductivity in superionic α-CuI [30]. In Figure 7, the interstitial self-diffusivity in pure Ni measured from ab-initio-based molecular dynamics is compared to the analytical value based on experimental resistivity recovery experiments. The agreement is reasonably good, in particular with respect to the activation energy.

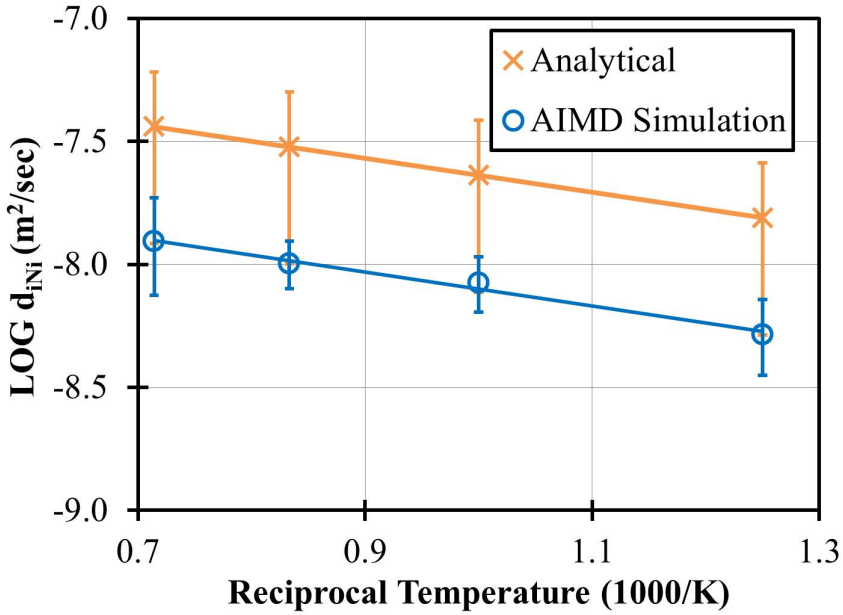

Figure 7: Interstitial self-diffusivity of pure Ni as a function of reciprocal temperature, as determined analytically and as measured from AIMD simulations. Temperatures range from 800 K to 1400 K. From [29].

The determination of interstitial diffusion coefficients will be particularly crucial for Mn; due to a lack of experimental data on RIS of Mn in stainless steels, computational methods will be necessary to determine a best estimate for the sign and magnitude of Mn segregation. Once the

vacancy and interstitial diffusion coefficients for Mn are obtained, they can be used in a readily available rate theory RIS model to make such an estimate [31].

An additional area in which atomistic calculations can be utilized in the proposed modeling plan is in the determination of precipitate-matrix interfacial energies. This is a necessary input parameter for CNT simulations, however a precise value is generally unknown. Once likely precipitate phases have been determined via CALPHAD, DFT can be used to calculate interfacial energies either by interface construction in a slab calculation or by embedding a particle of the precipitate phase in an austenite matrix and calculating the total energy relative to the separate bulk phases.

4. SUMMARY OF PROPOSED MODELING PLAN

The proposed modeling plan is show schematically in Figure 8. First, the CALPHAD framework will be utilized to determine the equilibrium phase separation of Mn-Ni-Si rich phases from the austenite matrix, using the best available description of the thermodynamics of the Fe-Cr-Ni-Mn-Si alloy system. The resulting predicted compositions and volume fractions of the second phases will be compared to the precipitate phases observed experimentally after irradiation. This approach will demonstrate whether the experimentally observed phases reflect the equilibrium state of the alloy or if they are strictly induced by the irradiation.

If it is determined that the precipitate phases are reflective of the equilibrium phase separated state, then CNT simulations will be performed to estimate the time scale of the Mn-Ni-Si rich precipitate nucleation, growth, and coarsening under thermal aging conditions. If the predicted time scale is drastically different from experimentally observed precipitation under irradiation, then irradiation-enhanced diffusion will be introduced into the CNT simulations to determine whether this factor alone can account for the enhancement of the precipitation under irradiation. If the experimentally observed precipitate phases do not reflect the phase separation predicted by CALPHAD, then it is possible that the precipitation is induced by the irradiation, rather than only enhanced by it. One plausible mechanism by which the irradiation might induce precipitation is RIS, which can dramatically alter alloy composition in certain regions of the material. RIS data, experimentally measured diffusion coefficients, and ab-initio calculations will then be utilized to estimate this change in alloy composition. The CALPHAD model will then be used to determine whether this change in composition might result in the precipitation of an unexpected second phase.

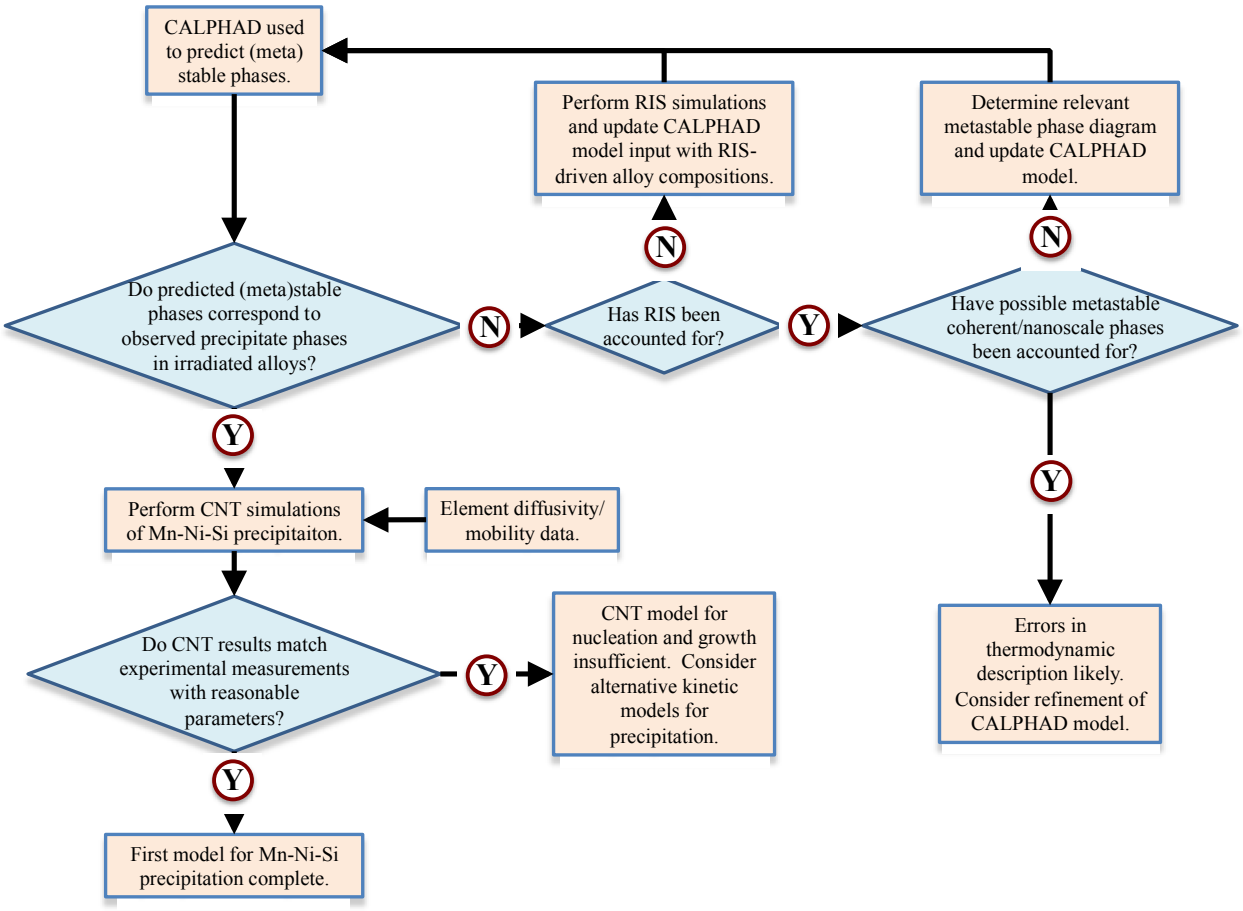

Figure 8: Logical schematic of proposed thermokinetic modeling plan.

Throughout this process the computational methods described above will be used to supplement and refine model parameters as necessary. The computational tools and resources necessary to implement this modeling plan are in place and accessible, with the exception of the Thermo-Calc software. The purchase of the Thermo-Calc software package is expected to cost approximately $22,000. This is a one-time fee that will include the TCAL2 database, the associated mobility database MOBAL2 for the calculation of concentration dependent chemical diffusion coefficients, and the Dictra and TC-Prisma modules, which are used to implement the CNT simulations.

5. BIBLIOGRAPHY

[1]R.M. Boothby, D.R. Harries, T.M. Williams, J Nucl Mater, 115, (1983), 16-24

[2]H.R. Brager, F.A. Garner, J Nucl Mater, 108, (1982), 347-358

[3]E.H. Lee, L.K. Mansur, J Nucl Mater, 278, (2000), 20-29

[4]P.J. Maziasz, J Nucl Mater, 169, (1989), 95-115

[5]P.J. Maziasz, J Nucl Mater, 205, (1993), 118-145

[6]W. Xiong, G.R. Odette, D. Morgan, (To be submitted 2013),

[7]F. Christien, A. Barbu, J Nucl Mater, 324, (2004), 90-96

[8]A.J. Ardell, in: V. Ghetta, D. Gorse, D. Maziere, V. Pontikis (Eds.) Materials Issues for Generation IV Systems, Springer, 2008, pp. 285.

[9]Y. Yang, Private Communication, in, 2013.

[10]B. Jonsson, Scandinavian Journal of Metallurgy, 24, (1995), 21-27

[11]J. Ruzickova, B. Million, Mat. Sci. & Eng., 50, (1981), 59-64

[12]B. Jonsson, Z Metallkd, 86, (1995), 686-692

[13]J. Kucera, B. Million, K. Stransky, Kovove Mater, 41, (2003), 325-334

[14]T.P.C. Klaver, D.J. Hepburn, G.J. Ackland, Phys Rev B, 85, (2012),

[15]M.T. Malik, D. Bergner, Cryst Res Technol, 23, (1988), 1503-1515

[16]D. Bergner, Y. Khaddour, S. Loerx, Defect and Diffusion Forum, 66-69, (1989), 1407-1412

[17]J. Arunkumar, C. David, K.G.M. Nair, B.K. Panigrahi, C.S. Sundar, Adv Mater Sci Eng, (2012),

[18]C. Dimitrov, O. Dimitrov, Journal of Nuclear Materials, 152, (1988), 21-29

[19]T.R. Allen, G.S. Was, Acta Materialia, 46, (1998), 3679-3691

[20]E.A. Kenik, J Nucl Mater, 187, (1992), 239-246

[21]K. Fukuya, K. Fujii, Journal of Nuclear Science and Technology, 46, (2009), 744-752

[22]B. Hu, H. Takahashi, H. Itoh, T. Takeyama, Acta Metallurgica Sinica, 3, (1990), 229-235

[23]N. Metropolis, A.W. Rosenbluth, M.N. Rosenbluth, A.H. Teller, E. Teller, J. Chem. Phys. , 21, (1953),

[24]D. de Fontaine, Solid State Physics, 34, (1979),

[25]D. de Fontaine, in: H. Ehrenreich, D. Turnbull (Eds.) Solid State Physics, Academic Press, New York, 1994, pp. 33.

[26]J.M. Sanchez, F. Ducastelle, D. Gratias, Physica A, 128, (1984),

[27]A.R. Allnatt, A.B. Lidiard, *Atomic Transport in Solids*, Cambridge University Press, 1993.

[28]B. Sahli, W. Fichtner, Physical Review B, 72, (2005),

[29]L. Barnard, D. Morgan, Journal of Nuclear Materials, (submitted 2013),

[30]C.E. Mohn, S. Stolen, S. Hull, J Phys-Condens Mat, 21, (2009),

[31]L. Barnard, J.D. Tucker, S. Choudhury, T.R. Allen, D. Morgan, Journal of Nuclear Materials, (2011),